R&PA

N

N-99818

Technical Report No. 32-104

The Plasma Core Reactor

D. F. Spencer

jpl
JET PROPULSION LABORATORY
CALIFORNIA INSTITUTE OF TECHNOLOGY
PASADENA, CALIFORNIA

April 24, 1961

NATIONAL AERONAUTICS AND SPACE ADMINISTRATION
CONTRACT NO. NASw-6

Technical Report No. 32-104

The Plasma Core Reactor

D. F. Spencer

R. R. McDonald

R. R. McDonald, Chief
Engineering Research Section

JET PROPULSION LABORATORY
CALIFORNIA INSTITUTE OF TECHNOLOGY
PASADENA, CALIFORNIA

April 24, 1961

CONTENTS

FIGURES

ABSTRACT

A preliminary analysis of the plasma core reactor concept, as applied to a rocket booster, indicates that the potential for such a system is great, provided certain technical problems can be solved. The analysis points out the important physical quantities which enter into the design of such a system and suggests specific areas which will require further investigation. In particular, experimental verification of axial confinement is necessary to prove the system technically feasible. Also, theoretical and experimental studies of the energy transport from the fissionable plasma to the propellant are required.

I. INTRODUCTION

The plasma core reactor is one which utilizes a gaseous fissionable material, probably plutonium, at a temperature sufficiently high to completely ionize the fissionable species, thus allowing interaction with electric and/or magnetic fields. If sufficiently high concentrations of the fissionable species can be obtained and maintained in a closed region (cavity) commensurate with certain time restrictions, the reactor will "go critical" and produce power. If this power is then absorbed in a propellant, e.g. hydrogen, the fission energy may be converted to kinetic energy of the propellant by exhausting it through a conventional deLaval nozzle to produce thrust. A theoretical limitation restricts exhaust velocity to approximately 30 km/sec. This limitation arises from the direct deposit in the chamber walls of a fraction of the fission energy, in neutron and gamma heating (Ref. 1).

Since the fissionable material is in a gaseous state, there are no such structural limitations as occur in the solid core nuclear rocket (Ref. 2). Thus, a very high core power density may be employed without destruction of the fuel. Such a device can therefore produce high thrusts accompanying the high exhaust velocities, provided the fission energy can be transported to the propellant.

It seems appropriate to discuss the merits of such a system in relation to other advanced high thrust propulsion systems, in particular, the fusion rocket (Ref. 3) and the pulse nuclear rocket.[1]

The plasma core reactor has two very important advantages over the fusion reactor. Probably the most basic is simply the fact that fission reactors have been operated over extended periods of time, while, to date, a sustained fusion reaction has not been demonstrated. Thus, from the standpoint of the availability date, it appears that such a device could precede the fusion rocket.

There is another very fundamental advantage of the plasma core reactor over the fusion device. In fusion, as is well known, the main source of power loss is the emission of bremstrahlung (X-rays) from the plasma. Since, in fusion, ion densities are limited to 10^{14} — 10^{15} particles/cm^3 (to maintain the pressure within reasonable limits), these X-rays penetrate the plasma and deposit their energy exterior to it. Thus, in order to balance this power loss, very high operating temperatures ($50\text{-}300 \times 10^{6}$ °K) are required.

As was mentioned previously, in the gaseous fission reactor concept, high fuel concentrations (later to be shown to lie between 10^{17} and 10^{19} particles/cm^3), are required for criticality. There of course, is still a very large bremstrahlung flux interior to the plasma; however, these X-rays are attentuated within the plasma due to its high atomic number, high concentration, and to the low energy of the X-rays. (The photoelectric absorption coefficient is proportional to Z^4/E^3; see Appendix.) Essentially, the only mode of energy transport from the plasma is that of thermal radiation from the plasma surface (neglecting for the moment γ emission and the kinetic energy of the neutrons). Thus, the prospect of sustained high-temperature operation appears feasible.

In comparison with the pulse nuclear rocket, there are two obvious advantages for the plasma core reactor. These are the lowering of atmospheric contamination and the smaller fuel inventory for the "cavity" reactor.

---

[1] Described in the classified literature; for example: T. B. Taylor, GAMD-837. General Atomics, San Diego, Calif., June 1959 (Secret).

In the plasma core reactor, most neutrons and a large fraction of the gammas are attenuated within the reflector-moderator and the pressure-vessel walls. Of course, in the pulse nuclear system, these radiations are not attenuated at all before entering the atmosphere. As will be discussed later, the plasma core reactor is inherently a high-thrust device, thus making possible Earth-surface launch with a high-specific-impulse vehicle giving significantly less external radioactivity than that of nuclear pulse vehicle.

Although the fuel is not reclaimed in either the plasma core or the pulse rocket, the smaller fuel expenditure for the plasma core rocket lowers the cost of such a device in addition to lowering atmospheric contamination.

This paper is primarily concerned with the technical problems basic to the realization of such a rocket system. There are three main areas which must be examined: (1) criticality of the gaseous fueled system, (2) confinement of the fissionable plasma for a sufficiently long period of time, and (3) the energy transport process from fuel to propellant. The major difficulty in the analysis of such a system stems from the interdependence of these areas. Although criticality of the plasma core reactor depends to some extent on the thermal balance, it can most easily be isolated from the system analysis. Thus, it will be considered first.

II. CORE CRITICALITY

If we anticipate the fact that very high plasma temperatures (2×10^4 to 10^5 °K) will be required, it becomes obvious that a chamber wall temperature as high as can be sustained is desired. This conclusion is reached if we consider the fact that approximately 10% of the generated energy is deposited in the solid wall and this thermal energy must be transferred to the propellant before injection into the "cavity". It is this enthalpy rise in the cavity walls which determines the theoretical specific impulse attainable, as is pointed out in Ref. 1.

The chamber wall must act as a reflector-moderator for the neutrons and also as a structural member for the system. With these restrictions in mind, graphite appears to present the best compromise; thus this analysis is based on its use.

The maximum operating temperature of graphite is approximately 2500°K, which corresponds to an average energy for the neutrons of 0.32 ev. This is the center of a fairly broad resonance of plutonium; therefore calculations in this Report will be based on this energy and a plutonium-fueled core.

In order to alleviate major computational problems, a number of simplifying assumptions will be made.

1. Fixed ions (in actual fact, the fuel ions may have velocities comparable to the "thermalized" neutrons).
2. Spherical symmetry of the plasma core (the actual core is a quasi-sphere because of the closing of the magnetic field at either end of the cylindrical plasma with $L/D \approx 1$).
3. No upscattering in energy of the neutrons by the propellant (the mean free path is very long in hydrogen so this should be a good assumption).
4. No absorption by the propellant (this should not be too important for pressures up to 30 atmospheres).
5. The Reflector-moderator is graphite, with a uniform temperature of 2500°K and an effectively infinite thickness (1 - 2 meters).

6. Cross sections are evaluated at $E = 0.32$ ev except for graphite. It is assumed to have its room-temperature absorption cross section for conservatism.

7. The fuel only absorbs thermalized neutrons.

8. No gap between core and reflector moderator (the space which would be occupied by the propellant).

Since the problem is restricted to that of purely external moderation and based on the preceding simplifying assumptions, we may apply the analysis given by Safonov (Ref. 4).

The critical equation in this case is:

$$3\gamma_c = \left[f\eta \left(\frac{4\pi a^2}{3} \right) \phi_V(a) - \left(\frac{\phi_p(a)}{-l\,\phi_p'(a)} \right) \right]^{-1} \tag{1}$$

where the symbols are as defined in the nomenclature following this Section.

The flux at the core-moderator interface is:

$$\phi_V(a) = \frac{3L^2}{4\pi (L^2 - a^2)\, l a} \left\{ e^{\tau/a^2} \left(1 - erf\, \frac{\tau^{1/2}}{a} \right) \right.$$

$$\left. + \tfrac{1}{2}\, e^{\tau/L^2} \left[(1 - a/L) \left[1 + erf \left(- \frac{\tau^{1/2}}{L} \right) \right] - (1 + a/L) \left(1 - erf\, \frac{\tau^{1/2}}{L} \right) \right] \right\} \tag{2}$$

and

$$\frac{-\phi_p'(a)}{l\,\phi_p'(a)} = \frac{a/l}{1 + a/L} \tag{3}$$

Once we have determined the value of γ_c the solution given by Safonov yields:

$$3\,\gamma_c \approx B\left(1 - \frac{B^2}{6}\right) \tag{4}$$

where

$$B = \Sigma_a^{29}\, a \tag{5}$$

We proceed by determining the invariants in the calculations, i.e. the nuclear parameters for core and reflector. The microscopic cross-sections which were utilized are taken from BNL 325, 2nd ed. (Ref. 5), and are listed below:

$$\sigma_a^{29} = 4 \times 10^3 \text{ b}$$

$$\sigma_f^{29} = 2.5 \times 10^3 \text{ b}$$

$$\sigma_a^{\mathrm{Gr}} = 3 \text{ mb}$$

$$\sigma_s^{\mathrm{Gr}} = 4.8 \text{ b}$$

Next, the pertinent nuclear parameters for the criticality analysis are determined:

Pu^{239}	Graphite
$\nu = 2.88 \quad \eta f = 1.8$	$l = 2.67$ cm
	$L^2 = 3.58 \times 10^3 \text{ cm}^2$
	$\tau = 2.2 \times 10^2 \text{ cm}^2$

A range of values of the parameter a, the critical radius, must be assumed. From Safonov, the range of interest should lie between 75 and 200 cm. Thus, we select a = 75, 100, 150, and 200 cm for computational purposes.

The critical greyness γ_c may now be determined, and from it are obtained the critical concentration n and the critical mass M. These parameters are given as a function of critical radius in Fig. 1 and 2.

Thus, from this analysis, the range of fuel concentrations which must be confined is fixed. The next section will cover the important considerations of the confinement problem.

Nomenclature (Section II)

a	core radius = core moderator boundary, cm
B	dimensionless parameter
$erf\,(x)$	$= 2\sqrt{\pi} \int_0^x e^{-y^2} dy$
f	thermal utilization of fuel, dimensionless
L/D	length to diameter ratio of fuel, dimensionless
L	thermal diffusion length in reflector-moderator, cm
l	thermal transport mean free path in reflector-moderator, cm
M	fuel mass, kg
n	fuel concentration, particles/cm^3
γ_c	critical greyness, dimensionless
η	average number of neutrons released per neutron absorbed in fuel, dimensionless
ν	average number of neutrons per fission, dimensionless
Σ_a^{29}	macroscopic absorption cross section for plutonium 239, cm^{-1}
σ_a^{Gr}	microscopic absorption cross section for graphite, barns
σ_a^{29}	microscopic absorption cross section for plutonium 239, barns
σ_f^{29}	microscopic fission cross section for plutonium 239, barns
σ_s^{Gr}	microscopic scattering cross section for graphite, barns
τ	neutron age in reflector moderator material, cm^2
$\phi_p\,(a)$	thermal neutron flux at $r = a$ arising if entire sphere were made of moderator material, neutrons/cm^2 sec
$\phi'_p\,(a)$	gradient of thermal neutron flux at $r = a$ if entire sphere were made of moderator material, neutrons/cm^3 sec
$\phi_V\,(a)$	thermal neutron flux in reflector moderator material at $r = a$, neutrons/cm^2 sec

III. PLASMA CONFINEMENT

The most basic problem underlying the plasma core reactor is that of confining the high-temperature fissionable species in a closed region away from the chamber walls for a sufficiently long time. In cylindrical geometry, this entails containment in both the radial and axial directions.

A simple approach to the problem would suggest the possible use of a static electric field. Experimental results (Ref. 6) yield the following equation relating the maximum space-charge density attainable to the applied voltage and cell geometry:

$$\rho = \frac{\epsilon_0^V}{Z_0^2} \tag{6}$$

For argument purposes, we select an electrode spacing of 0.2 meters and an impressed voltage of 2×10^5 volts. Then the maximum space charge density which can be confined is 1.77×10^{-4} coulombs/m^3. If we assume the fuel atoms to be singly ionized, the charge per ion is merely 1.6×10^{-19} coulombs.

The maximum concentration which may be confined is given by:

$$n = 6.25 \times 10^{12} \rho = 1.1 \times 10^9 \text{ particle/cm}^3 \tag{7}$$

This, of course, is far below that required for a critical assembly, thus eliminating the possible use of only a static-electric field to produce confinement.

The next approach is to consider the use of a strong external magnetic field to confine the plasma. It is known that at very low densities, a homogeneous steady magnetic field will produce radial confinement of a plasma for periods of hours; however, extrapolation to plasmas of higher densities is difficult.

The containment problem may be separated into two important geometrical considerations -- radial and axial confinement of the plasma. This analysis is based on the use of the so called "mirror geometry" proposed by Post (Ref. 7).

This entails the use of a magnetic mirror which "reflects" the ions in the axial direction. However, to enhance the axial confinement, an internal magnetic field is induced in the plasma. This field then limits both axial and radial diffusion losses since the field lines close within the plasma. The mirror geometry produces further confinement after the plasma "leaks" through the induced field (Fig. 3).

Confinement of the plasma may also be examined according to the loss mechanism, i.e. diffusion or instability losses. The latter subject will not be discussed. The difficulties involved in obtaining solutions to the transport equations are so numerous that theoretical and experimental results may disagree by many orders of magnitude. In particular, containment studies employing the mirror geometry have produced confinement times 10^5 times larger than those predicted theoretically (Ref. 8). In the mirror geometry, complications arise mainly due to the penetration of the field lines into the plasma, negating the assumption of a defined plasma boundary.

The principal loss of the fuel is due to collisions within the plasma and subsequent diffusion of the ions toward the chamber walls. In most applications, the plasma is assumed collisionless; thus particle orbit theory may be applied to determine relaxation times for the plasma.

In order to utilize particle orbit theory, the product of the mean collision time and the gyration frequency of the particles should be of order 1 or greater. These variables are given by:

$$\tau_i = \lambda_i / \bar{v}_i \tag{8}$$

$$\lambda_i = \frac{1}{n_i \, \sigma_i} \tag{9}$$

$$\sigma_i = \frac{3.59 \times 10^{-5}}{T_P^2} \tag{10}$$

$$\bar{v}_i = \left(\frac{3k \, T_p}{m_i} \right)^{1/2} \tag{11}$$

$$\omega_i = \frac{e B}{m_i c} \tag{12}$$

Then,

$$\tau_i\, \omega_i = \frac{1}{3.59 \times 10^{-5}} \frac{e}{c} \frac{B}{n_i} \frac{T_P^{\,3/2}}{(3k\, m)^{1/2}} \tag{13}$$

Since criticality considerations require ion concentrations of 10^{17} – 10^{19} particles/cc, the only remaining variables at our disposal are the plasma temperature and applied magnetic field strength. If we select magnetic field strengths of 10^4 to 10^6 gauss, the plasma temperature corresponding to $\tau_i\, \omega_i = 1.0$ may be determined. These temperatures are tabulated below for a critical concentration, 2.7×10^{17} ions/cm^3. Higher fuel concentrations, of course, require higher plasma temperatures for the same magnetic field strength.

B gauss	T_P °K
10^4	8.3×10^6
10^5	1.8×10^6
10^6	3.9×10^5

Thus fuel temperatures of 3.9×10^5 °K or greater are required if the plasma is to be effectively collisionless at the fuel concentrations of interest. Since the power radiated at these temperatures is exorbitantly high it is necessary to restrict attention to a collision-dominated plasma, and/or to allow some fission heating in the chamber walls (thus lower fuel concentration in the plasma).

A. Radial Confinement

At this time the analysis is limited to the collision dominated case of radial diffusion loss of the plasma. The loss mechanism is dependent on the rate at which the colliding ions can migrate to the chamber walls. Assume a plasma boundary has been obtained by some compression and/or injection mechanism. Let us then consider the rate of loss of the plasma, with the following assumptions:

1. The plasma is isothermal and completely ionized (a good assumption for plutonium above 10^4 °K).

2. The plasma is singly ionized and electrically neutral.

3. Only radial motion is considered.

4. Only a constant axial magnetic field is present.

5. The plasma is collision-dominated.

6. Particles have an isotropic, Maxwellian distribution of velocities.

7. Any propellant which may surround the plasma core is neglected (the propellant case will be considered next).

The diffusion equation in cylindrical co-ordinates is:

$$- D_j \left(\frac{\partial^2 \phi_j}{\partial r^2} + \frac{1}{r} \frac{\partial \phi_j}{\partial r} \right) = \frac{\partial \phi_j}{\partial t} \tag{14}$$

In the steady state, for the ions,

$$- \frac{D_i}{r} \left[\frac{d}{dr} \left(r \frac{d\phi_i}{dr} \right) \right] = 0 \tag{15}$$

whose solution is

$$- D_i \left(\frac{d\phi_i}{dr} \right) = C = - J_r = - \phi_i v_r \tag{16}$$

$$\phi_i = n_i v_r \tag{17}$$

$$D_i \left(v_r \frac{dn_i}{dr} + \cancelto{0}{n_i \frac{dv_r}{dr}} \right) = (n_i v_r) v_r \tag{18}$$

and we have the familiar equation,

$$D_i \frac{dn_i}{dr} = n_i v_r \tag{19}$$

The radial diffusion velocity is then

$$v_r = \frac{D_i}{n_i} \frac{dn_i}{dr} \tag{20}$$

The diffusion coefficient of the ions in the presence of a magnetic field may be shown to have the the form (Ref. 8):

$$(D_i)_0 = \frac{(D_0)_i}{1 + (\tau_i \omega_i)^2} \tag{21}$$

where

$$(D_0)_i = \frac{\lambda_i \bar{v}_i}{3} \tag{22}$$

and τ_i and ω_i are as given previously. Similar equations apply to the electrons, but since they have higher velocities for a given plasma temperature, they are lost more readily than the ions. If these ambipolar effects are taken into account (Ref. 9),$D_i \approx 2\,(D_i)_0$.

The concentration gradient is assumed constant in the radial direction and is given approximately by n_i/a.

A range of plasma temperatures from 2×10^4 to $10^5\,^\circ$K is selected for the analysis. The ions are so highly collision-dominated that the external magnetic field does not substantially inhibit diffusion; thus the diffusion coefficient is

$$D_i \simeq \frac{2\lambda_i \bar{v}_i}{3} \tag{23}$$

Now, the radial diffusion velocity of the plasma is

$$v_r = \frac{D_i}{n_i} \frac{n_i}{a} \tag{24}$$

Then the relaxation time of the plasma in the radial direction is approximately

$$t_i \simeq a/v_r \tag{25}$$

The following tabulation presents the ion diffusion coefficient, radial diffusion velocity, and radial relaxation time as a function of plasma temperature for a fuel concentration of 2.7×10^{17} ions/cm^3:

T_P °K	D_i cm^2/sec	v_r cm/sec	t_i sec
2×10^4	4.0	1.3×10^{-2}	1.0×10^4
5×10^4	4.0×10^1	1.3×10^{-1}	1.0×10^3
10^5	2.2×10^2	7.4×10^{-1}	2.0×10^2

These values of t_i indicate that sufficient retention of the plasma will be maintained radially if the plasma can originally be forced into a critical volume. Since the magnetic field does not inhibit radial diffusion substantially, it acts mainly as a trapping mechanism to provide the original plasma (fuel) boundary.

We now consider the more appropriate case where the diffusion of the fuel ions into the hydrogen is considered. It is assumed that ion-atom collisions are identical to atom-atom collisions. Only ion diffusion is considered i.e. ambipolar effects are neglected.

The diffusion coefficient of the fissionable species (indicated by subscript 1) into the propellant (indicated by subscript 2) is given (Ref. 10) by:

$$D_{12} = \frac{n_1 \lambda_2 \bar{v}_2 + n_2 \lambda_1 \bar{v}_1}{3(n_1 + n_2)} \tag{26}$$

where:

$$\lambda_1 = \frac{1}{\pi n_2 r_{12}^2 \left[1 + \left(\frac{\bar{v}_2}{\bar{v}_1}\right)^2\right]^{1/2}} \tag{27}$$

with a similar equation for λ_2

$$r_{12} \approx 3.2 \times 10^{-8} \text{ cm} \tag{28}$$

$$\bar{v}_1 = \sqrt{\frac{2k\bar{T}_1}{m_1}} \tag{29}$$

$$\bar{v}_2 = \sqrt{\frac{2k\bar{T}_2}{m_2}} \tag{30}$$

The hydrogen is assumed to have an average temperature of 1.2×10^4 °K and average pressure of 30 atm. Then the number of particles per cm^3 of hydrogen, n_2, is 4.0×10^{19}.

Now,

$$n_1 \lambda_2 \approx \frac{1}{\pi r_{12}^2} = 3.1 \times 10^{14} \text{ particle/cm}^2 \tag{31}$$

From the form of the diffusion equation, it may be seen that for fuel densities less than 10^{19} per/cm^3, the diffusion coefficient is not sensitive to changes in plasma concentration. Thus we consider $n_1 = 2.7 \times 10^{17}$ ions/cm^3. The diffusion coefficient, radial diffusion velocity, and relaxation time of the plasma (radially) are given below:

T_P °K	D_{12} cm^2/sec	v_r cm/sec	t_i sec
2×10^4	3.7	1.2×10^{-2}	2.5×10^4
5×10^4	3.7	1.2×10^{-2}	2.5×10^4
10^5	3.8	1.3×10^{-2}	2.3×10^4

The main difference in the confinement time is due to the fact that the hydrogen acts as a restraining wall for the plasma; thus, the diffusion rate does not vary substantially with fuel concentration or plasma temperature. The important point is that radial confinement times sufficient for boost-vehicle applications appear realizable.

B. Axial Confinement

It has been pointed out by Kolb (Ref. 11) that the trapping of a magnetic field within the plasma can substantially increase axial confinement times in the mirror geometry. If we discharge a capacitor bank to produce a rising external magnetic field, an electric field is induced within the plasma from Faraday's Law.

$$\nabla \times \mathbf{E}_i = \mu_0 \frac{\partial \mathbf{H}_e}{\partial t} \tag{32}$$

In the following argument, the external magnetic field is assumed to be only in the axial or z direction; however, the analysis predicts to within an order of magnitude the axial confinement time of the plasma if it is assumed that an external magnetic field, which forms a plasma with $L/D \approx 1$, can be produced.

Following the analysis presented in Ref. 12, it can be shown that

$$\frac{1}{r}\frac{\partial}{\partial r} r\,(E_\phi)_i = \mu_0 \frac{\partial (H_z)_e}{\partial t} \tag{33}$$

This induced electric field gives rise to an internal current density and, in turn, an internal magnetic field whose flux lines close within the plasma, thus producing the enhanced axial confinement.

From Ohm's Law,

$$(j_\phi)_i = \sigma\,(E_\phi)_i \tag{34}$$

and

$$\nabla \times \mathbf{H}_i = \mathbf{i}_i \tag{35}$$

or

$$\frac{-\partial (H_z)_i}{\partial r} = (j_\phi)_i \tag{36}$$

It is the time for this field to decay which determines the axial confinement time for the plasma. Thus,

$$\frac{\partial (\mathbf{H})_i}{\partial t} = \eta\,\nabla^2 (\mathbf{H})_i \tag{37}$$

where:

$$\eta = (4\pi\mu_0)^{-1} \tag{38}$$

The transverse electrical conductivity σ is given by Ref. 13 as

$$\sigma = \frac{8 \times 10^{-3}\, T_p^{\,3/2}}{\ln \Lambda} \tag{39}$$

For a cylindrical plasma with $L \approx D$,

$$t_d = \pi \mu_0 \sigma D^2 \tag{40}$$

The axial relaxation time of the plasma is tabulated below for two typical densities and three plasma temperatures.

T_p °K	σ mho/m	t sec
$n_i = 1.1 \times 10^{18}$ ions/cm^3, $D = 2$ meters		
2×10^4	3.8×10^3	6×10^{-2}
5×10^4	1.5×10^4	2.4×10^{-1}
10^5	4.2×10^4	6.6×10^{-1}
$n_i = 2.7 \times 10^{17}$ ions/cm^3, $D = 4$ meters		
2×10^4	3.8×10^3	2.4×10^{-1}
5×10^4	1.5×10^4	9.6×10^{-1}
10^5	4.2×10^4	2.6

It is thus evident from this analysis that axial confinement times due to the induced field are too small to retain the fuel within the cavity throughout the boost period. If we now superimpose the loss time of the plasma out of the magnetic mirror with no trapped field, an estimate of the total confinement time can be made.

For a collision-dominated plasma, Ref. 11 gives the following equation for the axial relaxation time:

$$\tau_e = \tau_s \, 2 \left(\frac{A_p}{A_m} \right) \frac{\dfrac{L}{v_i}}{\dfrac{16 \, T_p^{3/2}}{n \ln \Lambda}} \tag{41}$$

For a plutonium plasma between 2×10^4 and 10^5 °K, and a magnetic-mirror ratio of 10, this equation has the form:

$$\tau_e = 2 \times 10^{-1} \frac{L}{T_p^{1/2}} \tag{42}$$

Values of the axial relaxation time due to the magnetic mirror, τ_e and the sum of τ_e and t are presented below for the same critical densities as above where the length of the plasma is approximately equal to the plasma diameter.

T_P °K	τ_e sec	$\tau_e + t$ sec
$n_i = 1.1 \times 10^{18}$ ions/cm^3, $L = 200$ cm		
2×10^4	2.8×10^{-1}	3.4×10^{-1}
5×10^4	1.8×10^{-1}	4.2×10^{-1}
10^5	1.3×10^{-1}	7.9×10^{-1}
$n_i = 2.7 \times 10^{17}$ ions/cm^3, $L = 400$ cm		
2×10^4	5.6×10^{-1}	8.0×10^{-1}
5×10^4	3.6×10^{-1}	1.3
10^5	2.6×10^{-1}	2.9

From this analysis, it appears that the axial confinement time of the plasma is insufficient for booster application. This, however, may not be the maximum attainable confinement time. If very large surface currents can be induced in the plasma boundary (between the external and internal magnetic fields), a local heating of the plasma may increase the electrical conductivity in this region and thus inhibit loss of the confining magnetic fields. Alternately the surface magnetic field may be continually increased (to some limiting value), maintaining static equilibrium in the plasma.

There is also a possibility of enhancing the axial confinement by controlling the injection velocity vector of the propellant and thus hydrodynamically aiding confinement.

Of course, implicit in the preceding argument is the fact that the external magnetic pressure must balance the internal magnetic pressure and the kinetic pressure. This then determines the magnitude of the required external magnetic field. The minimum external field required, i.e., for no trapped field, is given by

$$P = B_{min}^2 / 8\pi \tag{43}$$

where $P = (n_i + n_e)\, k\, T_P$ for an isothermal plasma.

Values of the minimum magnetic field, for $n_i = n_e = 2.7 \times 10^{17}$ ions/cm^3, are tabulated below.

T_P °K	B_{min} gauss
2×10^4	6.0×10^3
5×10^4	1.0×10^4
10^5	1.3×10^4

We now take a slightly different approach in considering the axial confinement. According to Ref. 2, gaseous fission systems are practical only if they provide a separation ratio (pounds of propellant per pound of fuel) of approximately 10^3.

In order to determine the separation ratio for this system, a critical concentration of 2.7×10^{17} ions/cm^3 or a critical mass of 7.9 pounds will be assumed. The average fuel flow rate must be sufficient to make up (1) the fuel lost due to relaxation of the plasma (assuming some type of pulse operation) and (2) the fuel burned in producing propulsive power. Average values of fuel-loss rate due to relaxation of plasma are given below.

T °K	$t + \tau_e$ sec	$\dot{w}_f$ lb/sec
2×10^4	8×10^{-1}	9.9
5×10^4	1.3	6.1
10^5	2.9	2.7

Thus in order to obtain a separation ratio of 10^3, the propellant weight flow rate must be 10^3 times the total fuel flow rate. Actual obtainable values based on these assumptions will be presented in Section V.

It is apparent that a critical area requiring further theoretical analysis and probably experimental verification is that of axial confinement. If it is impossible to obtain steady confinement throughout the boost phase, (which appears to be the case), then the problems associated with pulse operation should be considered in detail.

Nomenclature (Section III)

$\dfrac{A_P}{A_m}$	magnetic mirror ratio, dimensionless
a	radial coordinate at plasma boundary, cm
B_{min}	minimum value of magnetic induction, gauss
C	constant, particles/cm sec^2
c	velocity of light = 2.9979×10^{10} cm/sec
D	diameter of plasma, m
D_i	diffusion coefficient of ions, cm^2/sec
$(D_i)_0$	diffusion coefficient of ions in presence of magnetic field, cm^2/sec
D_j	diffusion coefficient of jth species, cm^2/sec
$(D_0)_i$	diffusion coefficient of ions without magnetic field, cm^2/sec
D_{12}	diffusion coefficient of species 1 into species 2, cm^2/sec
E_i	induced electric field in plasma, emu
E_{ϕ_i}	azimuthal electric field in plasma, emu
e	elementary charge of an electron = 4.802×10^{-10} stat coulomb
H_e	external magnetic field strength, emu
H_i	internal magnetic field strength, emu
$(H_z)_e$	external magnetic field strength in z direction, emu
$(H_z)_i$	internal magnetic field strength in z direction, emu
J_r	radial current of ions, ions/cm sec^2
j_i	induced current density in plasma, emu
$(j_\phi)_i$	induced azimuthal current density in plasma
k	Boltzmann constant = 1.380×10^{-16} erg/atom °K
L	length of plasma, cm

Nomenclature (Cont'd)

m_i	mass of ions, gm
m_1	mass of species 1, gm
m_2	mass of species 2, gm
n	fuel concentration, particles/cm^3
n_e	electron concentration, electrons/cm^3
n_i	ion concentration, ions /cm^3
n_1	particle concentration of species 1, particles/cm^3
n_2	particle concentration of species 2, particles/cm^3
P	kinetic pressure, dynes/cm^2
R	radial coordinate of vessel wall, cm
r	radial coordinate, cm
r_{12}	collision radius of species 1 and 2, cm
T_P	absolute temperature of plasma, °K
$\overline{T}_1$	average absolute temperature of species 1, °K
$\overline{T}_2$	average absolute temperature of species 2, °K
t	time, sec
t_d	time for diffusion of magnetic field lines into plasma, sec
t_i	relaxation time for radial diffusion of ions, sec
V	applied voltage, volts
$\overline{v}_i$	mean ion velocity, cm/sec
v_r	radial diffusion velocity of ions, cm/sec
$\overline{v}_1$	mean velocity of particles of species 1, cm/sec
$\overline{v}_2$	mean velocity of particles of species 2, cm/sec
z	axial co-ordinate, cm

Nomenclature (Cont'd)

Z_0	half width of electrode spacing, m
ϵ_0	permittivity of free space = 8.85×10^{-12} coulomb^2/Newton m^2
η	diffusion coefficient of magnetic field lines, cm^2/sec
Λ	dimensionless parameter
λ_i	mean free path of ions, cm
λ_1	mean free path of particles of species 1, cm
λ_2	mean free path of particles of species 2, cm
μ_0	permeability of free space = $4\pi \times 10^{-7}$ h/m
ρ	space charge density, coulomb/m^3
σ	transverse conductivity of plasma, mhos/m
σ_i	ion-electron collision cross section, cm^2
τ_e	axial relaxation time through magnetic mirror, sec
τ_i	mean ion collision time, sec
τ_s	mean scattering time in plasma, sec
ϕ_i	ion flux, particles/cm^2 sec
ω_i	gyration frequency of ions, cps
ϕ_j	flux of *j*th species, particles/cm^2 sec
ω_i	gyration frequency of ions, cps

IV. THERMAL ANALYSIS

Although the thermal analysis presented here is qualitative, it indicates the complexity of the energy-transport process. The problem is to achieve a direct interchange of thermal energy between the fissionable plasma core and the working fluid with a minimum of heat transfer to the walls. The analysis may be broken into three parts: (1) energy exchange between plasma and propellant, (2) energy exchange mechanisms within the propellant, and (3) energy exchange between propellant and chamber walls.

The working fluid is, of course, gaseous in the cavity, so that thermal conduction should play a minor role and can be neglected.

The convective exchange between plasma and propellant is difficult to estimate since it is dependent on the propellant velocity, density, etc.; however, it appears that the principal mode of energy transport will be that of direct radiant interchange. Here the cooling problem is similar to that taking place in stars wherein the energy is "driven" from the star interior to the surface (Ref. 14). Of course, we wish to minimize the energy transmitted through the propellant, so a major requisite of the working fluid is that it be opaque to thermal radiation in, at least, a portion of the temperature range from 2500 to 100,000°K.

If there is a range of temperatures over which the propellant is opaque, there will be little radiant transport within the propellant in this region. Here the dominant transport process should be convective exchange.

Finally radiant exchange from propellant to walls will dominate the transport picture if the lower end of the opaque temperature range is appreciably above the wall temperature (2500°K). In the steady state, to heat the propellant from the wall temperature to the range where it becomes opaque, injection of the cooler propellant into the opaque gas may be required. Then turbulent mixing will produce some average propellant temperature in the opaque temperature range.

There are a number of other characteristics which the propellant should exhibit. It should have a low average molecular weight in order to produce the maximum specific impulse for a given temperature, or, in other words, have a high enthalpy per unit mass on dissociation and/or ionization. It must, however, have a sufficiently high ionization temperature to minimize interaction with external magnetic fields. As pointed out in Ref. 11, in a collision-dominated plasma, the more energetic particles are lost more rapidly through the magnetic mirror. This also makes the use of a low-molecular-weight propellant desirable, since if it should become ionized, it would be lost from the chamber more easily than the fuel, assuming its temperature to be of the same order as that of the fuel.

The propellant must, also, be compatible with the reflector-moderator at 2500°K and should have a minimum influence on the nuclear characteristics of the core (unless doped with fuel or absorber for control purposes). This criterion requires a small absorption cross section for the propellant. The propellant should also be storable as a liquid to minimize propellant-tank weight and to allow pumping to the desired chamber pressure.

With these criteria in mind, two obvious choices are hydrogen and helium, although the use of the latter is limited by the storage problem. Therefore, although helium may offer some advantages, hydrogen will be considered in view of the preceding criteria.

Hydrogen becomes essentially opaque for path lengths of 20 cm at a pressure of 30 atm in the temperature range 10,000 to 25,000°K (assuming hydrogen is a grey gas), as may be seen from Fig. 4 (Ref. 15 and 16). Since hydrogen becomes ionized above 10,000°K at 30 atm pressure, the relative effects of hydrodynamic and magnetic forces on it must be considered to determine what portion of the hydrogen will be trapped by the magnetic field. Figure 5 is a schematic of the cavity region, indicating qualitatively the temperature profile through the hydrogen.

Hydrogen has a fairly low neutron-absorption cross section, and if reasonable path lengths (core-to-reflector) can be utilized, it should not significantly affect core criticality. The path length, of course, will be determined from the complete thermal analysis of the system. It certainly can be stored for sufficient periods of time, so that this criterion is not limiting.

Since the major drawback with hydrogen is its low absorptivity between 2000 and 6000°K, it may be necessary to seed it with a small amount of foreign material during startup. Possibly carbon black or similar particles could be carried by the hydrogen, thus increasing its apparent absorptivity (although at the same time, increasing the average molecular weight). Alternately, the injection of water vapor into the gaseous hydrogen is possible. Since the water molecule is unsymmetric, it exhibits an appreciable absorptivity in the range of interest. Further, it has the advantage that, once dissociated, its properties are similar to those of hydrogen. It also should be compatible with hydrogen and would increase the molecular weight only slightly. Of course, both of these methods must be analyzed in more detail, but they appear to offer a possible solution to the heat transfer problem during the startup period.

The energy transport process is thus a very complicated combination of radiative and convective mechanisms. In summary, the thermal analysis is complicated by the following factors:

1. Convection transfer from plasma to propellant and within the propellant.

2. Turbulent mixing effects.

3. Transfer not only of radiation but of the working fluid, i.e., matter flowing into and out of an incremental volume.

4. Necessity of maintaining, the exterior boundary (wall) at ~ 2500°K.

5. Sensitive temperature dependence of the physical properties of hydrogen.

With these qualitative arguments, the quantitative work will be delayed to a later analysis if it is found that sufficiently interesting confinement times can be realized.

V. SYSTEMS ASPECTS

There are, of course, many problems associated with the utilization of such a reactor in a propulsion system. The conceptual design of a single stage vehicle employing this concept is shown in Fig. 6. The following analyses are presented only to indicate the potential of such a system and to make a preliminary attempt to determine some of the important design considerations. Since a quantitative thermal analysis has not been made, it is impossible to predict vehicle performance, i.e., payload weight; however, a range of values for some of the important system parameters are presented to give some feel for the magnitude of these variables.

A. Performance

The following assumptions are necessary in order to make estimates for the magnitudes of some of the important parameters.

1. The fuel radiates with an emissivity calculated from Ref. 16, with no back emission from the propellant.
2. Plasma radius is 2 meters ($n_i = 2.7 \times 10^{17}$ ions/cm^3).
3. Plasma temperature range is from 2×10^4 to 10^5 °K.
4. δ represents the fraction of energy entering the reflector-moderator.
5. Thermal energy transported to walls is negligible.
6. Specific impulse is determined for equilibrium flow conditions in the nozzle and a pressure ratio, P_c/P_e, of 20:1 (Ref. 17).
7. An ideal velocity increment of 18,000 ft/sec (typical for booster application) is selected.
8. Initial acceleration of the vehicle is 1.25g.

Now, the total energy leaving the core is

$$Q = \epsilon_P \, \sigma \, A_P \, T_P^4 \tag{44}$$

where

$$\epsilon_P = \alpha \rho \, r_p \, , \qquad \epsilon_P \leq 1.0 \tag{45}$$

$$\alpha = (2.9 \times 10^{22}) \; \rho / T_p^{\;7/2} \tag{46}$$

The thrust may be determined from

$$F = \frac{I_{sp} \, P_{ex}}{1.885 \, \Delta \, H_c} \tag{47}$$

where

$$P_{ex} = 4.2 \times 10^{-6} \; Q \tag{48}$$

The reactor power is

$$P_r = \frac{P_{ex}}{(1 - \delta)} \tag{49}$$

The required propellant flow rate can be determined since we limit the reflector moderator temperature to 2500°K. Then

$$\dot{w}_p = \frac{(2.2 \times 10^{-6}) \, \delta \, Q}{(1 - \delta) \, \Delta \, H_s}$$

$$\Delta H_s = 10 \text{ kcal/gm atom} \tag{50}$$

then

$$\dot{w}_p = (2.2 \times 10^{-7}) \left(\frac{\delta}{1 - \delta} \right) Q \tag{51}$$

With this value of $\dot{w}_p$, the relation

$$F = I_{sp} \; \dot{w}_p \tag{52}$$

and Eq. (47), the enthalpy rise of the propellant in the cavity may be determined.

$$\Delta H_c = \frac{P_{ex}}{1.885\, \dot{w}_p} \tag{53}$$

This determines the average propellant temperature $\overline{T}_H$ and the theoretical specific impulse for the system.

To determine the burning time, we appeal to the ideal velocity equation

$$\Delta V = I_{sp}\, g_c \ln \frac{W_0}{W_{bo}} \tag{54}$$

From assumption (8), $W_0 = F/125$. Then

$$W_p = W_0 \left(1 - \frac{1}{e^{\Delta V / I_{sp}\, g_c}}\right) \tag{55}$$

and

$$t_b = W_p / \dot{w}_p \tag{56}$$

The reactor power output is dependent upon the average thermal flux in the core, the core volume, and the fuel material and concentration. All of these have been calculated except the average flux, which may be determined from

$$\overline{\phi} = \frac{10^6\, P_r\, c}{\Sigma_f\, V_f} \tag{57}$$

Once the average thermal flux is known, the mass of fuel burned can be determined from

$$(M_f)_b = 10^{-3}\,\Sigma_a\,\bar{\phi}\,V_f\,\frac{A\,t_b}{N_{R_0}} \tag{58}$$

The separation ratio R_s may be calculated from the fuel flow rate determined previously (see Section III-B) and the additional fuel expenditure due to burnup.

Then,

$$R_s = \frac{\dot{w}_f + 2.2\,(M_f)_{b/t_b}}{\dot{w}_p} \tag{59}$$

These system parameters are tabulated in Table 1 for plasma temperatures from 2×10^4 to 10^5 °K for three values of δ. Of particular importance is the effect of δ on the maximum specific impulse obtainable from the system. If 10% of the fission energy is deposited in the solid walls, the theoretical specific impulse is 1800 sec, but it is 3300 sec if only 3% of the fission energy is deposited in the walls. The minimum theoretical value of δ is 0.03 if only the kinetic energy of the neutrons is absorbed in the reflector-moderator, but more probably δ will be 0.05 or greater due to gamma absorption in the walls of the chamber.

The separation ratio is plotted as a function of plasma temperature and engine specific impulse in Fig. 7. This ratio is based on pulsed operation with a confinement time calculated in Section III-B. Should longer confinement times be attainable, the separation ratio would increase almost directly with this time.

If a separation ratio of 10^3 is selected for the system, and a specific impulse of 2500 sec, a plasma temperature of 30,000°K is necessary, with a resulting thrust level of approximately 15×10^6 lb and an average core flux of 3×10^{18} neutrons/cm^2 sec. The total fuel expenditure would be approximately 1600 kg which is not exorbitant.

A very preliminary estimate of the weight of the graphite reflector-moderator indicates it weighs approximately 2×10^6 lb. This should represent, by far, the heaviest components of the system. Thus accelerations greater than 1 g should certainly be attainable; in fact the first-stage payload/gross weight ratio should be approximately 0.6.

The main problem associated with pulse operation of the system appears to be one of reactor dynamics. Since the plutonium is continually being lost and replenished, the problem of maintaining steady-state criticality appears quite severe.

Another important result of the analysis is that the required plasma temperature for a $R_s \geq 10^3$ is in the range where hydrogen has a high absorptivity for thermal radiation. This indicates that thermal exchange from fuel directly to propellant can be effected.

B. Magnetic Coil

A second major aspect of the system is that of generating the required magnetic fields. A possible solution to this problem is by regeneratively cooling the coil with the cryogenic propellant. If hydrogen is used as the propellant, it could be pumped past the coil (which is embedded in the graphite), thus lowering coil resistivity.

If sufficiently low coil temperatures can be maintained, and provided critical magnetic field strengths are not attained, the coil may even be superconducting. Experiments with Nb_3Sn indicate it is superconducting up to 18°K (Ref. 18) and remains superconducting in magnetic fields up to 70,000 gauss at 4.2°K (Ref.19).

In addition to the limitations on the magnetic field strength, there is the problem of coil being heated by gamma radiation. This heat must then be transferred to the propellant along with the I^2R dissipation from the coil (if non-superconducting). Although the gamma heating will probably prohibit operation under superconducting conditions, regenerative cooling will certainly minimize power requirements to the coil.

There are many other problems such as pressure-vessel design, turbopump, nozzle cooling, etc., which are not peculiar to the plasma engine and although important, they will not be considered even though each area will require appreciable effort for adaptation to this system.

Nomenclature (Section V)

A	atomic weight of fuel = 239
A_p	surface area of plasma, cm^2
c	constant = 3×10^{10} fission/watt-sec
D	diameter of plasma, cm
e	base of natural logarithms
F	thrust, lbs
g_c	conversion factor, 32.2 ft $lb_{mass}/sec^2\ lb_{force}$
ΔH_c	enthalpy rise of propellant in cavity, kcal/gm atom
ΔH_s	enthalpy rise in propellant in passing through moderator, kcal/gm atom
I_{sp}	specific impulse of propellant, sec
$(M_f)_b$	mass of fuel burned, kg
N_{R_0}	Avogadro's number = 6.023×10^{23} atoms/mole
P_{ex}	power going into exhaust, Mw
P_r	total power produced in core, Mw
Q	thermal energy leaving plasma, cal/sec
r_p	radius of plasma boundary, cm
R_s	fuel separation ratio, lb propellant/lb fuel
T_p	plasma temperature, °K
t_b	burning time, sec
V_f	volume of fuel, cm^3
ΔV	ideal velocity increment, ft/sec
W_{bo}	burnout weight of vehicle, lb
W_0	initial weight of vehicle, lb
W_p	propellant weight, lb

Nomenclature (Cont'd)

$\dot{w}_f$ fuel flow out of magnetic field, lb/sec

$\dot{w}_p$ propellant flow rate, lb/sec

α opacity of plasma, cm^2/gm

δ fraction of fission energy deposited in solid, dimensionless

ϵ_p thermal emissivity of plasma, dimensionless

ρ plasma density, gm/cm^3

Σ_a macroscopic absorption cross section of fuel, cm^{-1}

Σ_f macroscopic fission cross section of fuel, cm^{-1}

σ Stefan-Boltzmann Constant = 1.365×10^{-12} cal/cm^2 sec °K^4

$\bar{\phi}$ average thermal neutron flux in the fuel, $neutrons/cm^2$ sec

Table 1. Summary of system parameters

T_p °K × 10^4	ϵ	Q cal/sec × 10^{11}	P_{ex} Mw × 10^5	δ	P_r Mw × 10^5	$\dot{w}_p$ lb/sec × 10^3	ΔH_c kcal/gm × 10^2	$\bar{T}_H$ °K × 10^4	I_{sp} sec × 10^3	F lb × 10^6	W_0 lb × 10^6	W_p lb × 10^6	t_b sec	$\bar{\phi}$ $\frac{\text{neutrons}}{\text{cm}^2\ \text{sec}}$ × 10^{17}	$(M_f)_b$ kg	$\dot{w}_f$ lb/sec	R_s × 10^2
2	1.0	1.1	4.6	0.10	5.1	2.7	0.9	1.0	1.8	4.9	3.9	1.1	400	6.8	0.98	9.9	2.7
2	1.0	1.1	4.6	0.05	4.9	1.3	1.9	1.5	2.5	3.2	2.6	0.52	400	6.5	0.94	9.9	1.3
2	1.0	1.1	4.6	0.03	4.7	0.75	3.3	1.9	3.3	2.5	2.0	0.3	400	6.2	0.89	9.9	0.76
5	1.0	43	180	0.10	200	110	0.9	1.0	1.8	200	160	43	400	270	39	6.1	170
5	1.0	43	180	0.05	190	50	1.9	1.5	2.5	130	100	20	400	250	36	6.1	79
5	1.0	43	180	0.03	190	29	3.3	1.9	3.3	96	77	12	400	250	36	6.1	46
10	0.2	140	590	0.10	650	340	0.9	1.0	1.8	610	490	130	400	860	120	2.7	1000
10	0.2	140	590	0.05	620	160	1.9	1.5	2.5	400	320	64	400	820	120	2.7	470
10	0.2	140	590	0.03	610	96	3.3	1.9	3.3	320	260	39	400	810	120	2.7	280

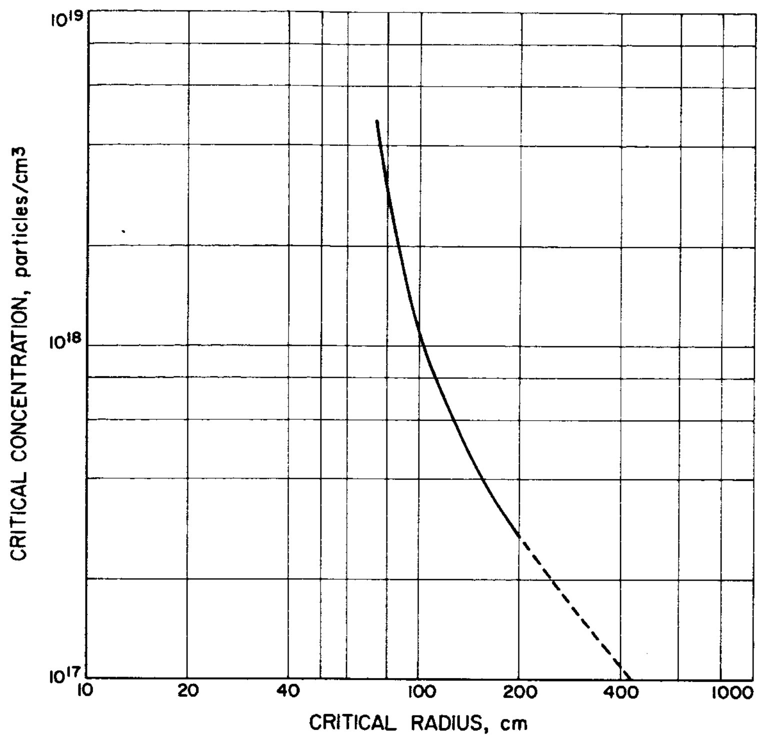

Fig. 1. Critical fuel concentration vs critical reactor radius

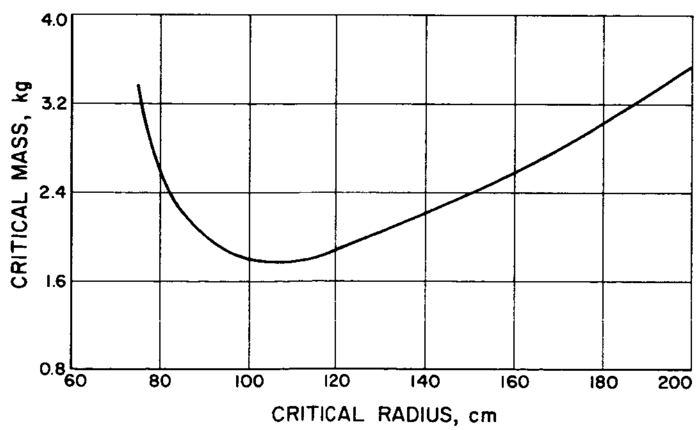

Fig. 2. Critical fuel mass vs critical reactor radius

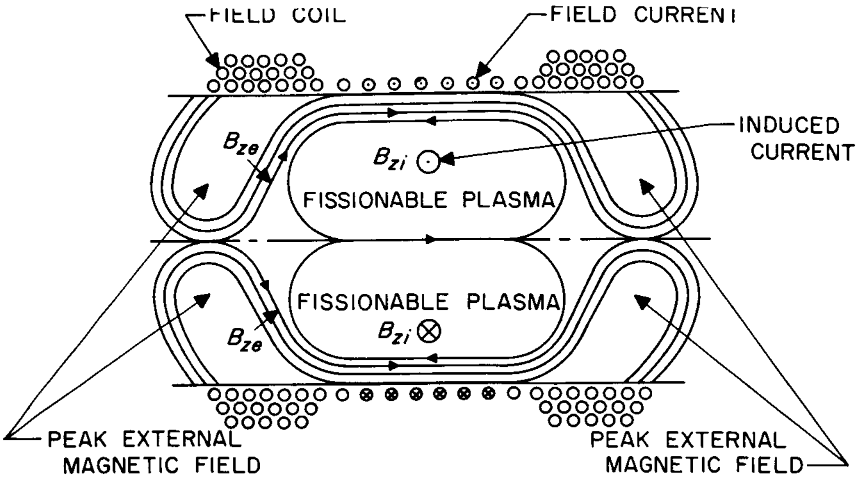

Fig. 3. Magnetic field configuration

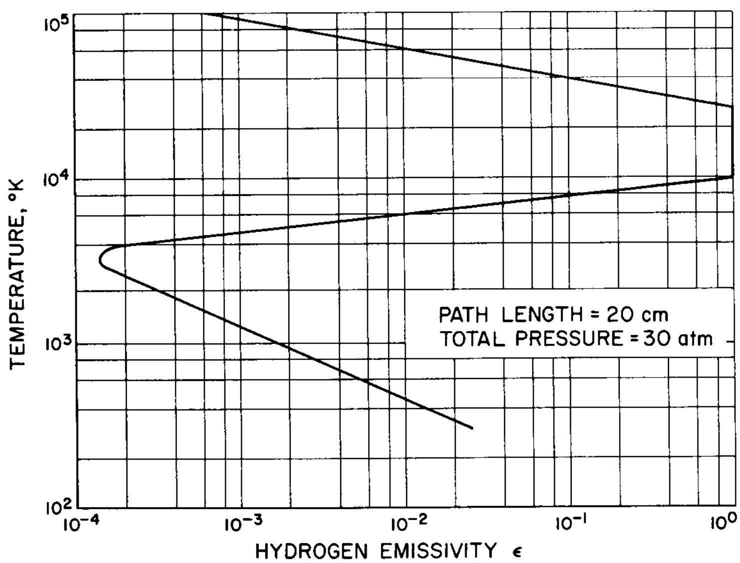

Fig. 4. Hydrogen emissivity vs temperature

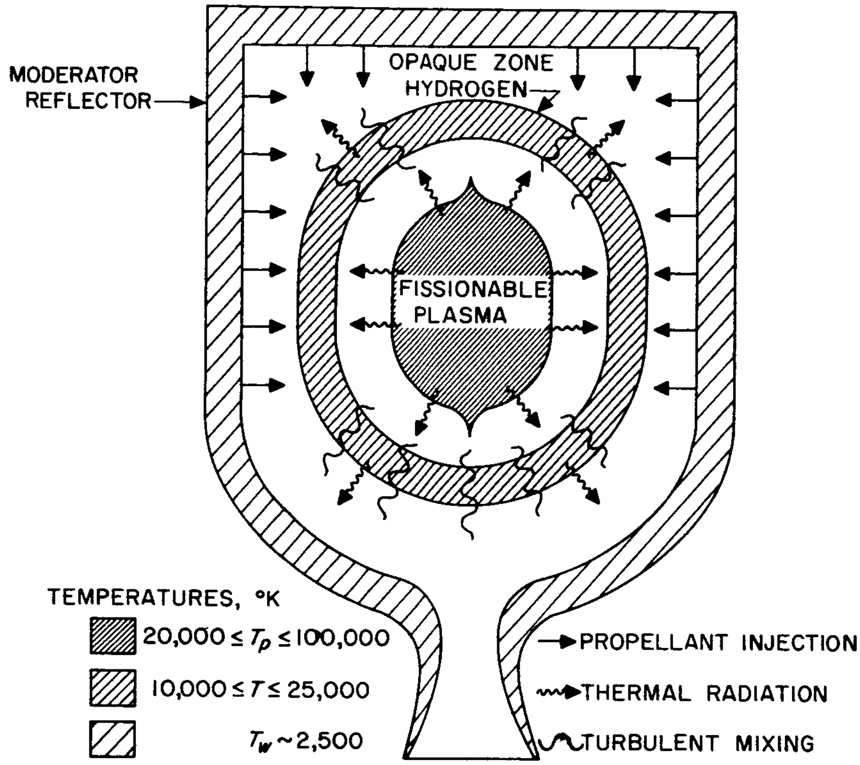

Fig. 5. Reactor temperature profile

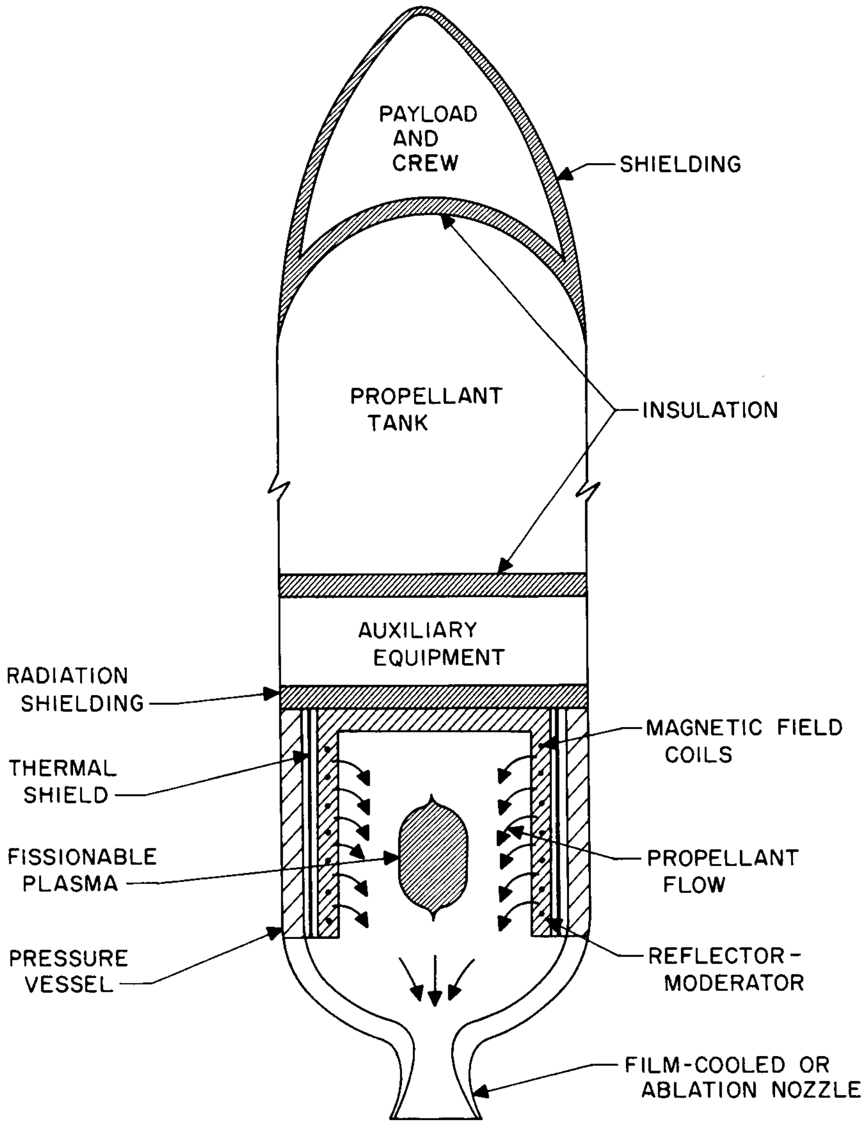

Fig. 6. Vehicle configuration

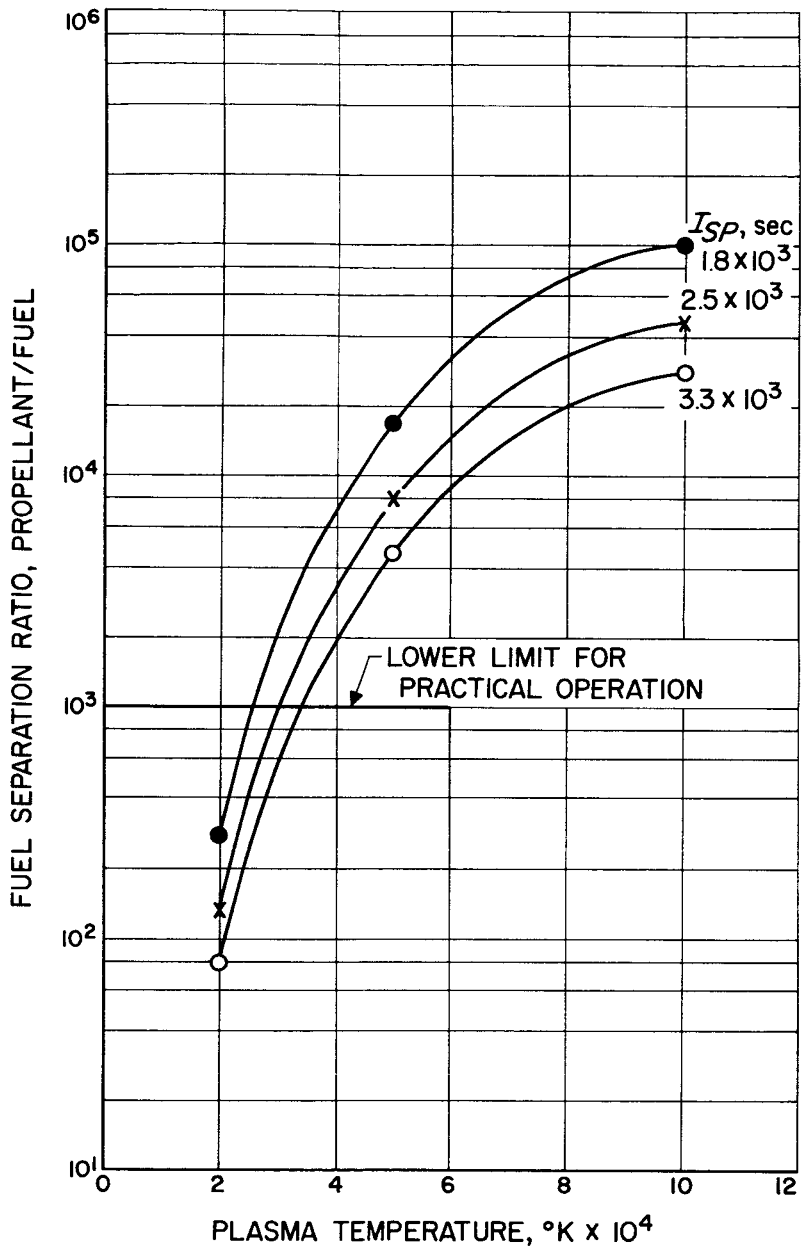

Fig. 7. Fuel separation ratio vs plasma temperature with engine specific impulse as a parameter

APPENDIX
Energy Transport from Plasma

This analysis shows that the bremstrahlung produced in the plasma are attenuated within it, so that the plasma loses energy mainly as thermal radiation.

From Ref. 19, the microscopic absorption cross section for the photoelectric effect is

$$\sigma_T = \frac{K Z^4}{E^3} \tag{A-1}$$

To evaluate K, the value of σ_T at $E = 1$ mev is obtained from the curves of Ref. 19.

$$\sigma_T \,\Big|_{(E = 1\ \mathrm{mev})} = (0.15 \times 10^{-32})\, Z^5$$

$$K = (0.15 \times 10^{-32})\, Z$$

If it is assumed that the electron loses all its kinetic energy in one encounter (the worst case), the bremstrahlung energy is given by

$$E = 3/2\, k\, T_P \tag{A-2}$$

For a plasma temperature of $10^5\,{}^\circ$K, $E = 1.3 \times 10^{-5}$ mev. The photoelectric absorption cross section of plutonium at this energy, from Eq. (A-1) is $\sigma_T = (5 \times 10^{-9})$ cm^2/atom. The macroscopic cross section is then

$$\Sigma = n_i\, \sigma_T \tag{A-3}$$

From Ref. 20, the power density of bremstrahlung in the plasma is:

$$P_b' = (0.54 \times 10^{-30})\, Z^2\, n_e^2\, (T_p')^{1/2} \tag{A-4}$$

Then the power emitted by a spherical plasma as bremstrahlung is

$$P_b = \int_0^{r_p} P_b' \, 4\pi r^2 e^{-\Sigma (r_p - r)} \, dr \tag{A-5}$$

For a uniform temperature and density in the plasma,

$$P_b = (6.8 \times 10^{-30}) \, Z^2 n_e^2 \, (T_p')^{1/2} \int_0^{r_p} r^2 e^{-\Sigma (r_p - r)} \, dr$$

If $\Sigma \, r_p >> 1$ and if Σ, in units of cm^{-1}, is greater than r_p^2 in cm^2, this equation can be integrated to give

$$P_b = (6.8 \times 10^{-30}) \, Z^2 r_e^2 \, (T_p')^{1/2} \frac{r_p^2}{\Sigma} \tag{A-6}$$

Now, the thermal power emitted by the plasma is

$$P_r \approx \epsilon \sigma \, A_p \, T_p^4 \tag{A-7}$$

For temperatures of approximately 5×10^4 °K and greater, the emissivity is given by (Ref. 15):

$$\epsilon = \frac{(2.9 \times 10^{22}) \, n_i^2 A^2 r_p}{(N_{R_0})^2 \, (T_p)^{7/2}} \tag{A-8}$$

The thermal power emitted is then

$$P_r = (2 \times 10^{-32}) \, n_i^2 A^2 (T_p')^{1/2} r_p^3 \tag{A-9}$$

Then the ratio of the thermal power emitted to the bremstrahlung power is

$$\frac{P_r}{P_b} = \left[\frac{(2.95 \times 10^{-3})\, n_i^2\, A^2\, (T_P')^{1/2}\, r_p^3}{n_e^2\, Z^2\, (T_P')^{1/2}\, r_p^2} \right] \Sigma \tag{A-10}$$

For electrical neutrality

$$n_i = n_e \tag{A-11}$$

and

$$\frac{P_r}{P_b} = (2.95 \times 10^{-3}) \left(\frac{A}{Z} \right)^2 r_p\, \Sigma \tag{A-12}$$

For a plutonium plasma at temperature, above $5 \times 10^4\,^\circ\mathrm{K}$, an ion concentration of 10^{17} ions/cm^3, and a plasma radius of 200 cm,

$$\frac{P_r}{P_b} = 1.9 \times 10^9 \tag{A-13}$$

Nomenclature (Appendix)

A atomic weight of fuel

A_p surface area of a spherical plasma, cm^2

E photon energy, mev

K constant, $mev^3\ cm^2/atom$

k Boltzmann constant = 1.38×10^{-16} erg/molecule °K

N_{R_0} Avogadro's number = 6.023×10^{23} atoms/mole

n_e electron number density, $electrons/cm^3$

n_i ion number density, $ions/cm^3$

P_b bremstrahlung power leaving plasma, watts

P_b' bremstrahlung power density in plasma, $watts/cm^3$

P_r thermal power leaving plasma, watts

r radial co-ordinate in plasma, cm

r_p radius of plasma boundary, cm

T_p plasma temperature, °K

T_p' plasma temperature, kev

Z atomic number of fuel

ϵ emissivity for thermal radiation

Σ macroscopic photoelectric absorption cross section, cm^{-1}

σ Stefan-Boltzmann constant = 5.67×10^{-12} $watts/cm^2\,°K^4$

σ_τ microscopic photoelectric absorption cross section, $cm^2/atom$

REFERENCES

1. *Gaseous Fission Reactors for Spacecraft Propulsion,* R. V. Meghreblian, Report No. 32-42, Jet Propulsion Laboratory, Pasadena, California, July 6, 1960.

2. *Nuclear Rocket Propulsion,* R. W. Bussard and R. D. DeLauer, McGraw-Hill Book Co., New York, 1958.

3. *Space Technology,* M. U. Clauser, John Wiley and Sons, Inc., New York, 1959, Ch. 18.

4. "Externally Moderated Reactors," G. Safonov, *Second United Nations International Conference on the Peaceful Uses of Atomic Energy,* Vol. 12, 1958, P. 705.

5. *Neutron Cross Sections,* D. J. Hughes and R. B. Schwartz, BNL 325, Brookhaven National Laboratory, Upton, New York, 2nd Ed., July 1, 1958.

6. *The Electrodynamic Containment of Charged Particles,* R. F. Wuerker, H. Shelton, and R. V. Langmuir, ERL-124, Ramo-Wooldridge Corp., Los Angeles, California, July 7, 1958.

7. "Summary of UCRL Pyrotron (Mirror Machine) Program," R. F. Post, *Second United Nations International Conference on the Peaceful Uses of Atomic Energy,* Vol. 32, 1958, p. 245.

8. "Stable Confinement of a High-Temperature Plasma," *Physical Review Letters,* Vol. 4, February 15, 1960.

9. *Controlled Thermonuclear Reactions,* S. Glasstone and R. H. Lovburg, D. Van Nostrand Co., New York, 1960.

10. *Gaseous Conductors,* J. D. Cobine, Dover Publications, Inc., New York, 1958.

11. "Magnetic Compression of Plasmas," *Reviews of Modern Physics,* Vol. 32, 1960, p. 748.

12. *Research Summary No. 36-7,* Jet Propulsion Laboratory, Pasadena, California, February 15, 1961, Vol. II, pp. 24-25. (Confidential).

13. *Physics of Fully Ionized Gases,* L. Spitzer, Jr., The Interscience Publisher, Inc., New York, 1956.

14. *The Atmospheres of the Sun and Stars,* L. H. Aller, The Ronald Press Company, New York, 1953.

REFERENCES (Cont'd)

15. *Equilibrium Emissivity Calculations for a Hydrogen Plasma at Temperatures up to 10,000°*K, D. Olfe, Technical Report No. 33, Guggenheim Aeronautical Laboratory, California Institute of Technology, Pasadena, California, May 1960.

16. "On the Problem of Cooling Atomic Rockets Which Utilize Thermonuclear Reactions,", H. J. Kaeppler, *Proceedings, Fourth International Congress on Astronautics,* Zurich, Switzerland, 1953. Translated by R. L. Bjork, T-53, The RAND Corporation, Santa Monica, California, November 1, 1955.

17. *Thermodynamic Properties and Calculated Rocket Performance of Hydrogen to 10,000°*K, D. Altman, Report No. 20-106, Jet Propulsion Laboratory, Pasadena, California, September 3, 1956.

18. "Superconductivity of Nb_3Sn," B. T. Matthias et al, *Physical Review,* Vol. 95, No. 6, September 15, 1954.

19. "Critical Field for Superconductivity in Niobium-Tin," B. M. Bozorth et al, *Physical Review Letters,* Vol. 5, No. 4, August 15, 1960.

20. *The Atomic Nucleus,* R. D. Evans, McGraw-Hill Book Company, Inc., New York, 1955.

21. "Controlled Fusion Research – An Application of the Physics of High Temperature Plasmas," R. F. Post, *Reviews of Modern Physics,* Vol. 28, No. 3, July 1956.